Electronic Supplementary Material (ESI) for Nanoscale.

Contrast Enhanced Ultrasound Imaging by Nature-Inspired Ultrastable Echogenic Nanobubbles

Al de Leon[1], Reshani Perera[2], Christopher Hernandez[2], Michaela Cooley[2], Olive Jung[2], Selva Jeganathan[2], Eric Abenojar[1], Grace Fishbein[3], Amin Jafari Sojahrood[3], Corey Emerson[4], Phoebe Stewart[4], Michael C. Kolios[3], Agata A. Exner[1,2,]*

[1]Department of Radiology, Case Western Reserve University, Cleveland, OH, 44106, USA
[2]Department of Biomedical Engineering, Case Western Reserve University, Cleveland, OH, 44106, USA
[3]Department of Physics, Ryerson University, Toronto, ON, Canada
[4]Department of Pharmacology, Case Western Reserve University, Cleveland, Ohio, 44106, USA

Supporting Information

Reagents (for 5 mL solution)	PG-PL	PG-Gly-PL	Gly-PL	PL
C22 (DBPC)	30.5 mg	30.5 mg	30.5 mg	30.5 mg
DPPA	5.0 mg	5.0 mg	5.0 mg	5.0 mg
DPPE	10.0 mg	10.0 mg	10.0 mg	10.0 mg
DSPE-mPEG 2000	5.0 mg	5.0 mg	5.0 mg	5.0 mg
PBS	4.0 mL	4.0 mL	4.0 mL	5.0 mL
Glycerol	**0**	**0.5 mL**	**1.0 mL**	**0 mL**
Propylene Glycol	**1.0 mL**	**0.5 mL**	**0 mL**	**0 mL**

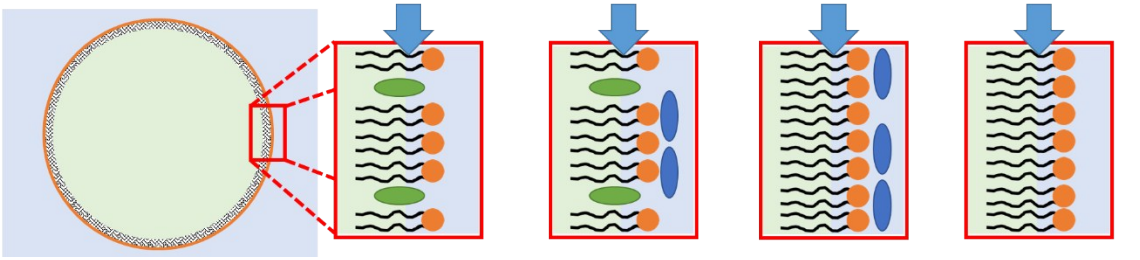

Table S1. Chemical composition of NBs and schematic representation of NB shell composition. The structure of PG-Gly-PL is formed through self-assembly of each component as dictated by their relative polarity with respect to the solvent and encapsulated gas. Phospholipid are amphiphilic molecules and therefore assembles at the C_3F_8-water interface with hydrophobic tail in contact with C_3F_8 gas and hydrophilic head in contact with water. Glycerol is a highly polar molecule with three –OH capable of forming hydrogen bonds with the hydrophilic phosphate head of phospholipid, while PG with its moderate polarity interacts with the middle part of the phospholipid connecting the hydrophobic tail and hydrophilic head.

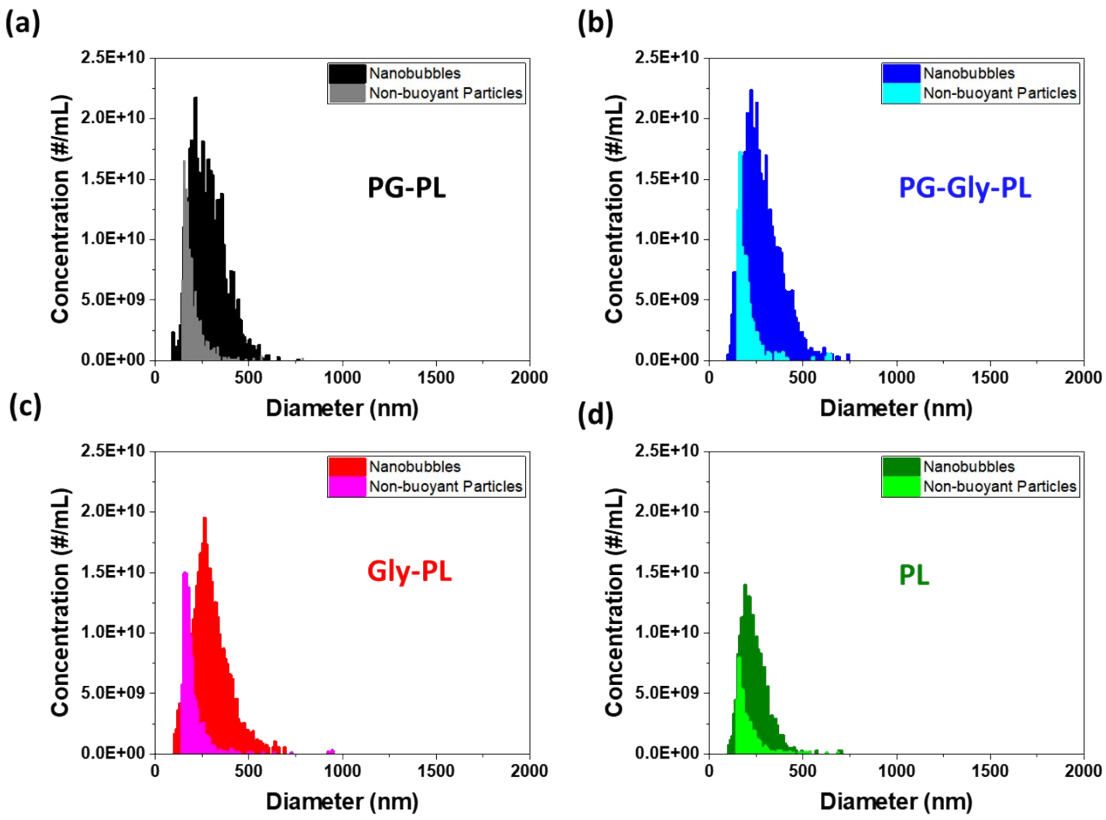

Figure S1. Particle size distribution of NBs and non-buoyant particles measured by resonant mass measurement.

Sample	Zeta Potential (mV)
PG-PL	-2.53 ± 0.88
PG-Gly-PL	-2.15 ± 1.78
Gly-PL	-2.04 ± 1.70

Table S2. Zeta potential of different NB solutions. Mean ± SE (n=3).

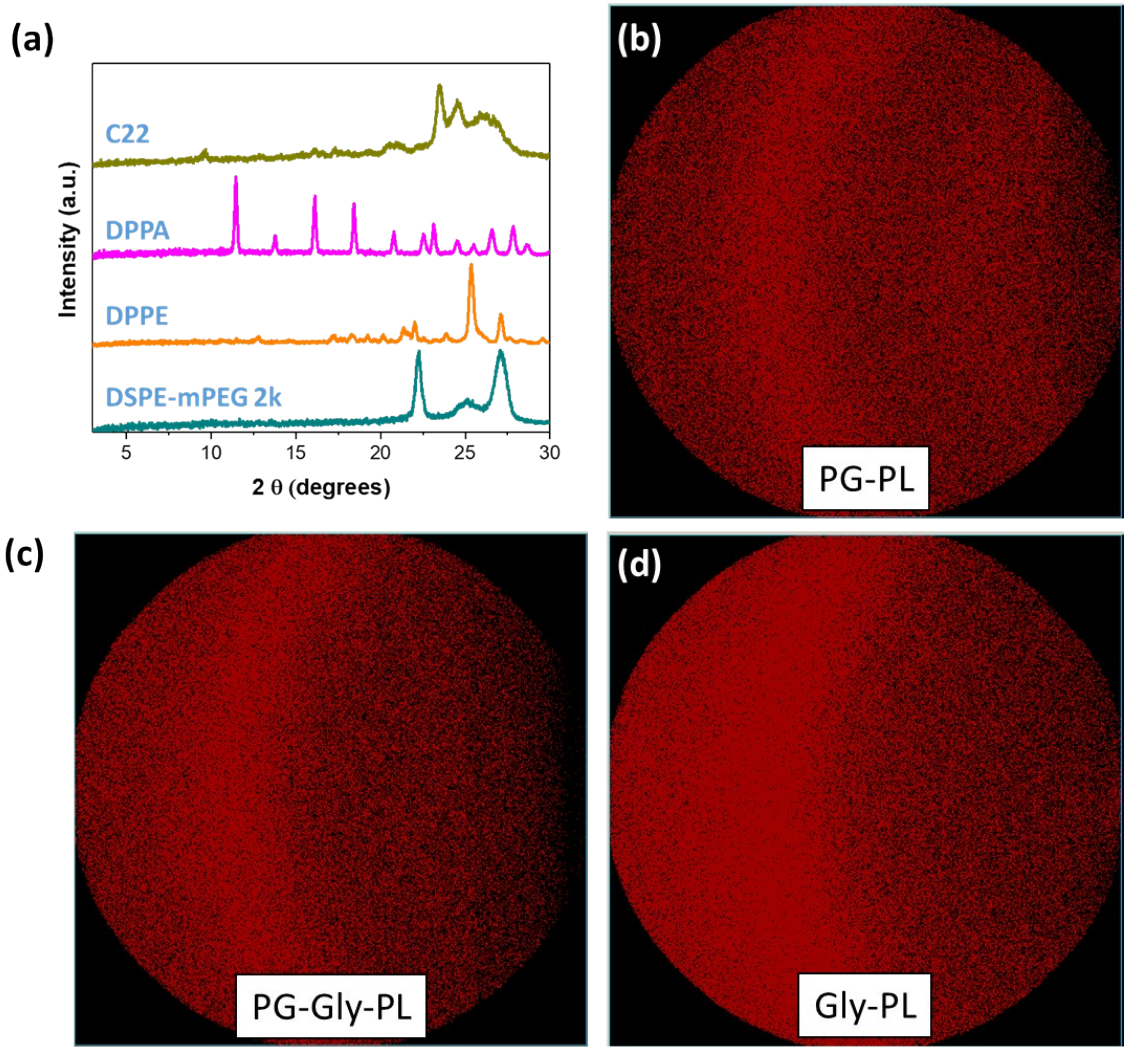

Figure S2. X-ray diffractograms of pure phospholipids used in the NB formulation and 2D XRD of freeze-dried NB membrane.

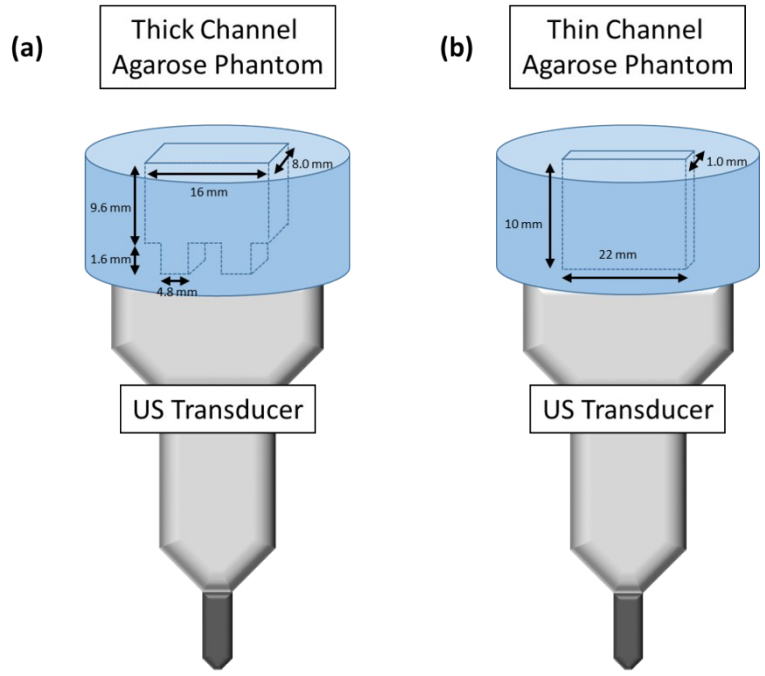

Figure S3. Schematic diagram showing the dimensions and orientation of the tissue-mimicking agarose phantoms used for echogenicity (a) and stability experiments (b).

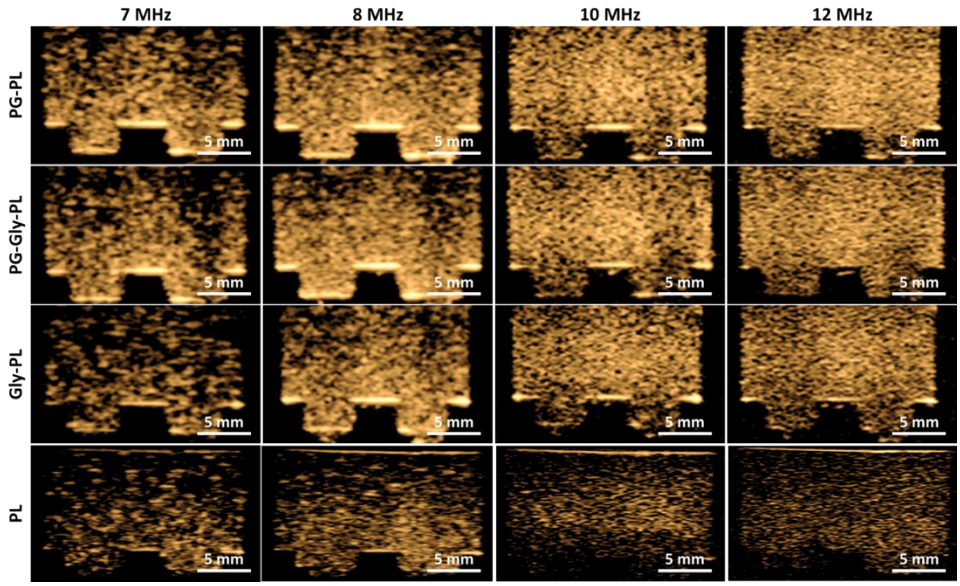

Figure S4. Ultrasound images captured in contrast harmonic imaging mode of NB solutions acquired at different frequencies.

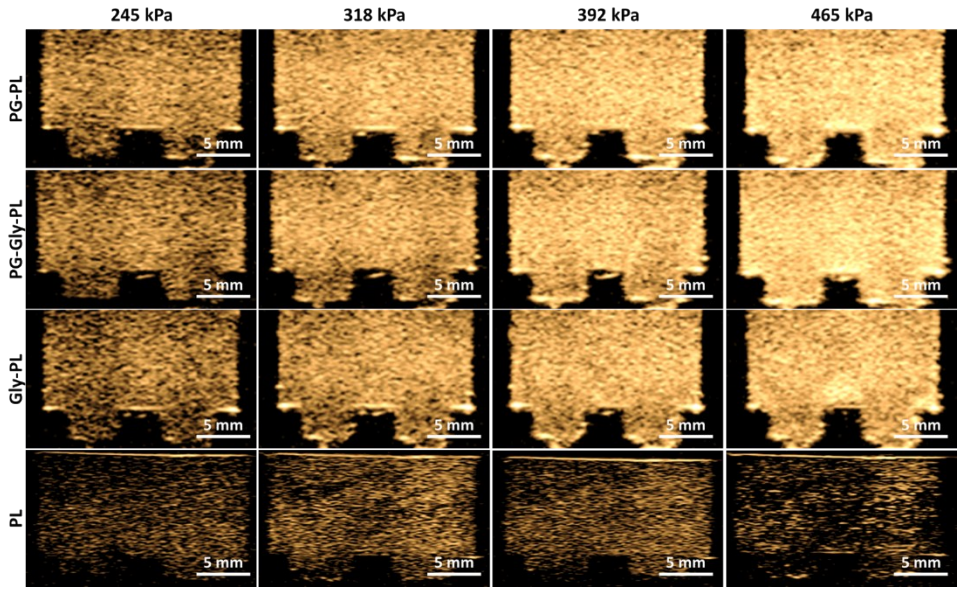

Figure S5. Ultrasound images captured in contrast harmonic imaging mode of NB solutions acquired at different peak negative pressures.

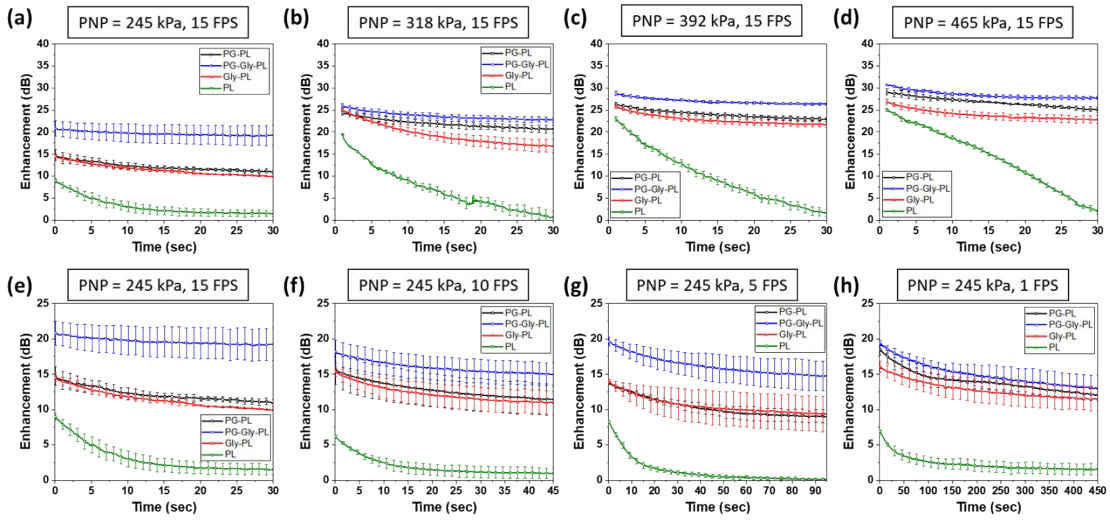

Figure S6. Stability curves of NB solutions acquired at different peak negative pressure and US pulse rate. Mean ± SE (n=3).

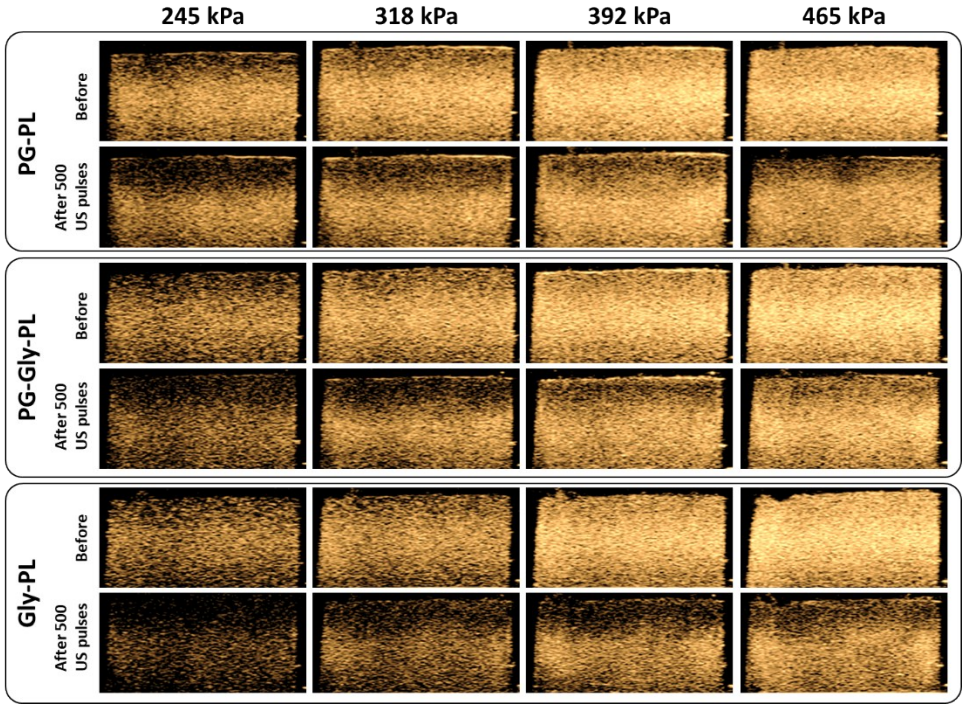

Figure S7. Ultrasound images captured in contrast harmonic imaging mode before and after exposure to 500 frames of varying peak negative pressures.

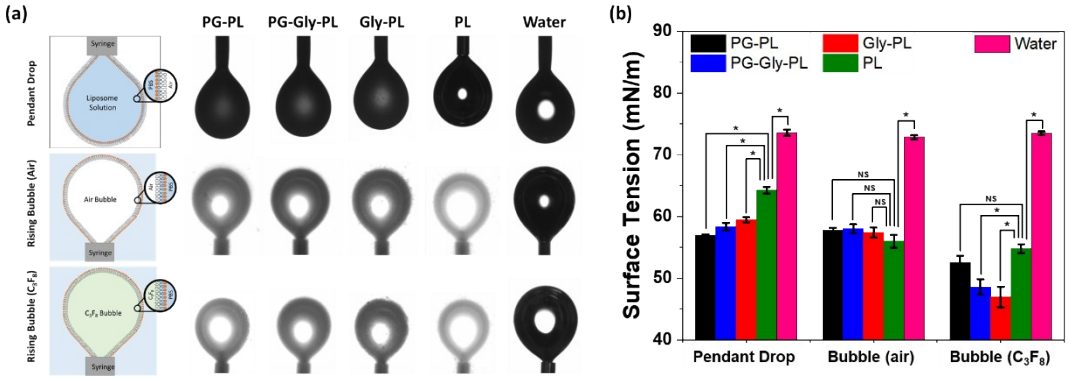

Figure S8. Surface tension measurement of NB solutions acquired via the pendant drop method, rising bubble method in air, and rising bubble method in C_3F_8. Mean ± SE (n = 3).

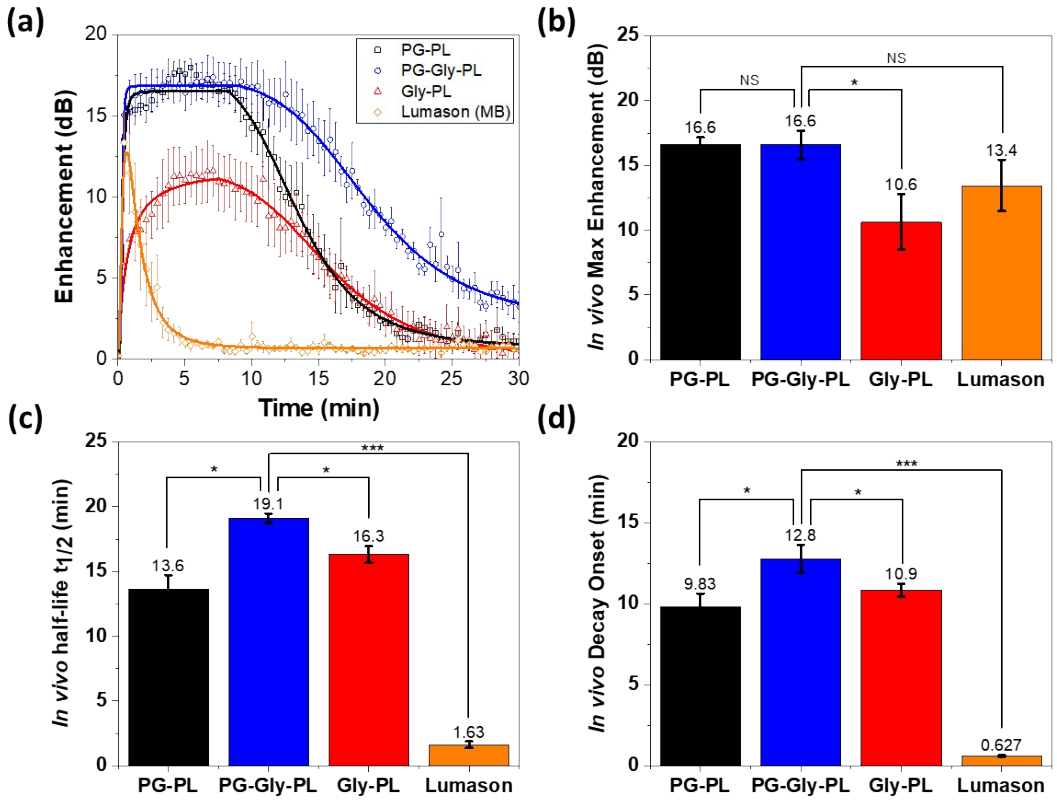

Figure S9. *In vivo* stability of NBs and Lumason in mouse liver showing similar behavior to that in the mouse kidney despite the presence of liver macrophages. Mean ± SE (n = 3)

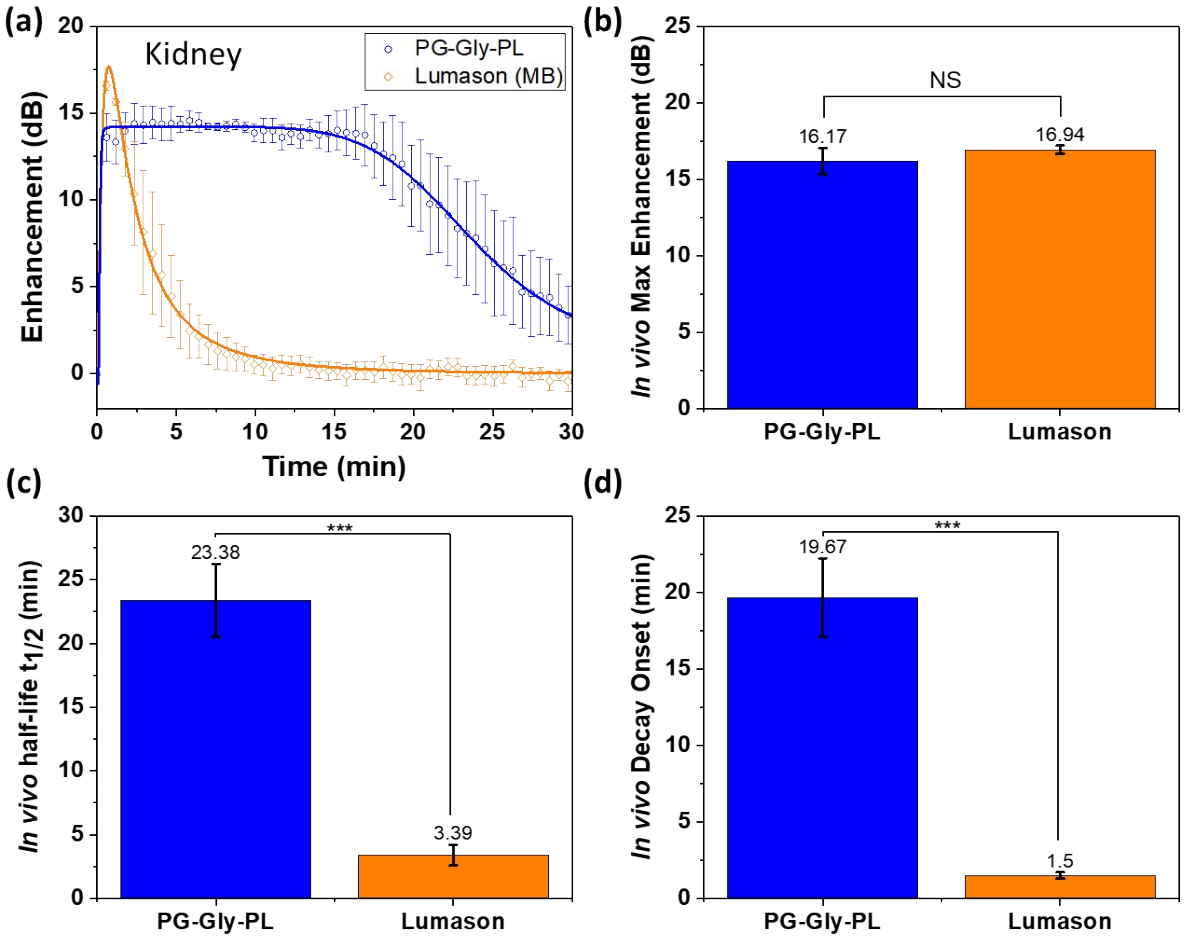

Figure S10. *In vivo* stability of PG-Gly-PL and Lumason in the kidney of a mouse with colorectal flank tumor. Mean ± SE (n = 3)

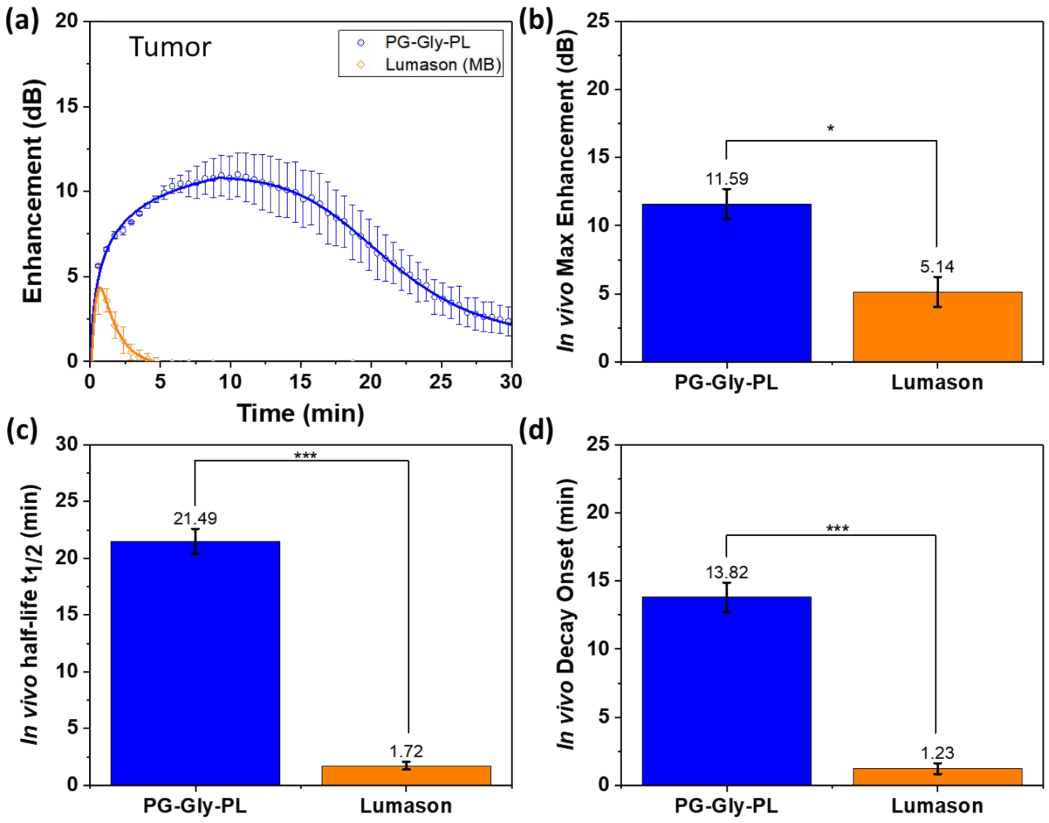

Figure S11. *In vivo* stability of PG-Gly-PL and Lumason in the colorectal flank tumor of a mouse. Mean ± SE (n = 3)